Biochemical Pharmacology 79 (2010) 610–622

Contents lists available at ScienceDirect

Biochemical Pharmacology

journal homepage: www.elsevier.com/locate/biochempharm

Heteronemin, a spongean sesterterpene, inhibits TNFα-induced NF-κB activation through proteasome inhibition and induces apoptotic cell death

Marc Schumacher [a,1], Claudia Cerella [a,1], Serge Eifes [a,1], Sébastien Chateauvieux [a], Franck Morceau [a], Marcel Jaspars [b], Mario Dicato [a], Marc Diederich [a,*]

[a] Laboratoire de Biologie Moléculaire et Cellulaire du Cancer, Fondation de Recherche Cancer et Sang, Hôpital Kirchberg, 9 Rue Edward Steichen, L-2540 Luxembourg, Luxembourg
[b] Marine Biodiscovery Centre, Department of Chemistry, University of Aberdeen, Meston Walk, Aberdeen AB24 3UE, Scotland, UK

ARTICLE INFO

Article history:
Received 24 July 2009
Accepted 30 September 2009

Keywords:
NF-κB
Marine natural product
Anti-cancer drug discovery

ABSTRACT

In this study, we investigated the biological effects of heteronemin, a marine sesterterpene isolated from the sponge *Hyrtios* sp. on chronic myelogenous leukemia cells. To gain further insight into the molecular mechanisms triggered by this compound, we initially performed DNA microarray profiling and determined which genes respond to heteronemin stimulation in TNFα-treated cells and which genes display an interaction effect between heteronemin and TNFα. Within the differentially regulated genes, we found that heteronemin was affecting cellular processes including cell cycle, apoptosis, mitogen-activated protein kinases (MAPKs) pathway and the nuclear factor κB (NF-κB) signaling cascade.

We confirmed *in silico* experiments regarding NF-κB inhibition by reporter gene analysis, electrophoretic mobility shift analysis and I-κB degradation. In order to assess the underlying molecular mechanisms, we determined that heteronemin inhibits both trypsin and chymotrypsin-like proteasome activity at an IC_{50} of 0.4 μM. Concomitant to the inhibition of the NF-κB pathway, we also observed a reduction in cellular viability. Heteronemin induces apoptosis as shown by annexin V-FITC/propidium iodide-staining, nuclear morphology analysis, pro-caspase-3, -8 and -9 and poly(ADP-ribose) polymerase (PARP) cleavage as well as truncation of Bid. Altogether, results show that this compound has potential as anti-inflammatory and anti-cancer agent.

1. Introduction

The number of identified natural compounds from marine sources has progressively increased especially in the field of anti-cancer research [1]. Besides, over 70% of earth surface is covered by the sea, which is the origin of life on earth and in some marine ecosystems, like coral reefs, the biodiversity is higher than in rain forests [2]. In recent years, a large number of natural products, with promising properties, have been isolated from marine sources, as reported in recent reviews [3]. In comparison to synthetic drugs, nature-derived drugs have various advantages, such as specific bioactivity and bioavailability, chemical structural diversity and the lack of toxic side effects. Besides, around 70% of all anti-cancer drugs used in clinical therapy were isolated from natural sources or bear a close structural relationship to compounds of natural origin [4].

Due to its implications in most incurable diseases, the nuclear transcription factor κB (NF-κB) has become one of the many investigated targets in drug discovery. Several pathways of activation have been described so far. The first elucidated and the most frequently investigated is the so-called canonical pathway, which can be triggered by external stimuli like TNFα. This pathway is mediated by the formation and translocation into the nucleus of the dimer p50/p65, upon phosphorylation and degradation of the cytoplasmic repressor I-κB protein [5]. This in turn contributes to the transcription of specific target genes [6]. The target genes play a role in several human diseases mainly linked to inflammation and cancer [7]. Besides, a close association between NF-κB and cancer exists. It has been published that inflammation is the main cause of cancer in 20% of cases [8]. In most cases, NF-κB is activated and closely associated to carcinogenesis. This is related to an ability of NF-κB to promote pro-survival pathways [9]; as supported by the fact that induction of apoptosis might follow the inhibition of the NF-κB pathway [10]. In addition, an aberrant NF-κB activity is responsible for resistance to chemo- and radiotherapy [11]. Thus, it is not surprising that the role of NF-κB signaling as a possible target for cancer therapy was discussed in recent reviews [12].

* Corresponding author at: Laboratoire de Biologie Moléculaire et Cellulaire du Cancer, Hôpital Kirchberg, 9 rue Edward Steichen, L-2540 Luxembourg, Luxembourg. Tel.: +352 2468 4040; fax: +352 2468 4060.
E-mail address: marc.diederich@lbmcc.lu (M. Diederich).
[1] Equally contributed.

0006-2952/$ – see front matter © 2009 Elsevier Inc. All rights reserved.
doi:10.1016/j.bcp.2009.09.027

Due to the higher susceptibility of cancer cells to treatments/agents affecting viability, the majority of anti-cancer therapies currently applied in clinics is based on cytocidal treatments, acting via apoptosis induction. Apoptosis is an active and highly regulated form of cell death by means of which damaged and mutated cells, potentially dangerous to the entire organism, can be eliminated. The execution of the apoptotic program may occur via the activation of different cascades of intracellular biochemical events converging in caspase-3 activation [13]. Two sets of events are commonly implicated in activating caspase-3: the extrinsic (or physiological) apoptotic pathway, triggered by stimulation of specific plasma membrane receptors (i.e., FAS) and mediated by caspase-8 activation; and the intrinsic (or mitochondrial) apoptotic pathway, which is triggered by stress-induced intracellular damages, leading to the release of cytochrome *c* from mitochondria and caspase-9 activation [14]. The two pathways are interconnected to amplify the apoptotic signal. Thus, caspase-8 can activate the mitochondrial pathway via truncation/activation of Bcl-2 family member Bid [15], whereas, caspase-8 can be further activated downstream to caspase-9 and -3 [16].

In the context of cancer and cancer therapy, DNA microarrays have been used so far for cancer classification [17] and to elucidate the potential mechanisms of action of cancer therapeutics respectively [18]. However, very few studies have focused so far on microarray technology for the functional profiling of natural compounds of marine origin as anti-cancer therapeutics [19].

In this study, we investigated the biological effects of the isolated marine spongean sesterterpene heteronemin on the resistant chronic myeloid leukemia cancer cell line K562. To gain insights into the molecular mechanisms of action of the compound, we performed DNA microarray profiling of the changes in the transcriptional program induced by heteronemin. We found that the compound was able to affect several cellular processes, including cell cycle, apoptosis, mitogen-activated protein kinases (MAPKs) pathway and the nuclear factor κB (NF-κB) activation cascade. The potential ability of the compound to potently inhibit NF-κB pathway and affect cell viability, as emerged from the DNA microarray profiling, was further confirmed by in vitro studies, thus showing heteronemin as a potent and promising inhibitor of TNFα-induced NF-κB activation as well as an apoptosis inducer.

2. Materials and methods

2.1. Heteronemin

A sample of *Hyrtios erecta* (phylum Porifera, class Demospongiae, order Dictyoceratida, family Thorectidae) was collected in November, 2000 from Vanuatu (15o 31.92′S, 167o 11.61′E) at a depth of 15 m, by Coral Reef Foundation scientists under contract with the US NCI. Collected material was stored at −20 °C until used. Voucher specimens are stored at the Smithsonian Institution, USA with voucher numbers 0CDN7710/C021264. The sample (sandy-green solid, 4.018 g dry weight) was extracted and partitioned as previously described [20]. The lipophilic hexane fraction was further purified on a normal phase silica HPLC-column (Phenomenex, Macclesfield Cheshire, UK) with hexane/ethyl acetate (70/30) solvent system to yield 180 mg of a white solid. This solid was identified as the sesterterpene heteronemin through its ^{1}H and ^{13}C NMR spectra by comparison to previously reported data in literature [21] (Fig. 1).

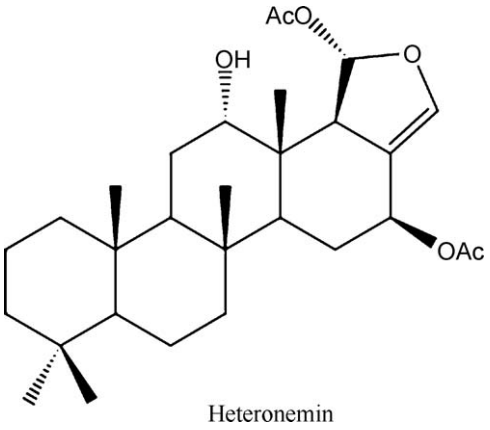

Fig. 1. Molecular structure of heteronemin.

2.2. Cell culture and treatment

Chronic myeloid leukemia K562 and Jurkat (T cell leukemia) cells were cultured in RPMI 1640 medium (Lonza, Verviers, Belgium) supplemented with 10% fetal bovine serum (Lonza), penicillin (100 units/ml) and streptomycin (100 μg/ml) (Lonza). Cells were cultured in a 5% CO_2 incubator at 37 °C and harvested every 3 days. For all experiments, we allowed 10 days, as the time needed to get enough cells after defrosting.

The day before treatment, four batches of cells are prepared for the control cells and treated cells in this way were not centrifuged on the day of treatment, thus avoiding a disruption in the transcriptome of cells undergoing short treatment. One hour before treatment, the cells are placed in the density of use. At T0, cells were treated with 4 μM of heteronemin or equivalent volume of DMSO. At T + 2 h, cells were treated with 20 ng/ml of TNFα, or equivalent volume of water. At T0 + 2 h 40 min cells were collected for RNA extraction and viability test. A control is performed in parallel for each processing time. RNA was extracted from a batch of 5–10^6 cells by the use of Trizol reagent (Invitrogen, Merelbeke, Belgium). RNA cleanup was performed by using the RNeasy Mini Kit (Qiagen, Venlo, Netherlands). RNA was quantified using a Nanodrop 1000 and the quality of this RNA was assessed by using the Agilent Bioanalyzer (RNA Integrity Number >9).

2.3. Microarray hybridization and feature extraction

Microarray experiments using Agilent 4112F human whole genome microarrays (Diegem, Belgium) were done according to the manufacturer's protocol with 700 ng of total RNA, isolated previously, used for the preparation of cDNA probe and the preparation of Cy5- and Cy3-labeled cRNA probes. The hybridized and washed material on each glass slide was scanned with an Axon 4100B microarray scanner (Sunnyvale, CA, USA). Axon GenPix Pro software version 6.1 was used for feature extraction.

2.4. Microarray normalization and analysis

Competitive microarray hybridizations were performed using a 2×2 factorial design, by comparing TNFα- and heteronemin-treated cells respectively to untreated control-cells, and heteronemin and TNFα co-treated cells relative to TNFα-treated cells alone. Experiments were performed in three biological replicates including two technical replicates. Technical replicates were hybridized as dye-swaps. Therefore each comparison corresponds to six hybridizations in total. The gene expression data were normalized and statistically analyzed using the R software package LIMMA (version 2.14.5) [22], which is part of the BioConductor project [23]. A linear model was fitted for the previously described experimental design. Additionally, the use of dye-swaps in the experimental setup allowed the estimation of a probe-specific dye-effect. This approach allows to remove dye-effect in the model and

so to improve precision for the detection of differentially expressed genes.

The background correction was performed using the "normexp" function [24] with an offset of 100. "normexp" is a method implemented in LIMMA which allows stabilizing the variability of log-ratios as a function of signal intensity. Subsequently global loess normalization [25] was performed on the resulting log-ratios using a span of 0.4 to eliminate intensity-dependent dye-bias. Probes without related Entrez Gene ID annotations were eliminated in a subsequent step. A moderated *F*-test was used to test the remaining spots for significant changes in expression. The following contrasts were tested: "TNFα vs. Control", "Heteronemin vs. Control" and the interaction effect between heteronemin and TNFα. It might be noteworthy that the interaction effect allows detecting for which genes heteronemin and TNFα show an antagonistic respectively synergistic effect on the respective RNA levels.

Array quality weighting, by using the gene-by-gene update algorithm [26] was used to improve the quality of statistical analysis. By using a relative weighting approach for array quality, one may increase the power of statistical analysis for differential expression of genes. Furthermore, spots flagged as "not found" by GenePix were down-weighted. The spot- and array-wise weights are then combined into modified weights for every spot, which are used as weights in the linear model for differential expression analysis.

The *p*-values were adjusted for multiple hypotheses testing by using the Benjamini–Hochberg false discovery rate (FDR) [27]. Only spots with a FDR <0.05 and showing at least a 1.5-fold change were considered as statistically significant. In case where more than one spot on the array was related to the same gene, only the most significant spot with the highest *F*-statistic was considered for further analysis.

2.5. Quantitative real-time RT-PCR

Reverse transcriptions were performed on the same batch than the microarrays. The reaction was performed on 5 μg of RNA with the SuperScript™ III first strand synthesis system for RT-PCR (Invitrogen).

Real-time PCR was performed on 25 ng of RNA equivalent, with the Mesa Green qPCR MasterMix Plus for SYBR® Assay (Eurogentec, Seraing, Belgium) according to the manufacturer's protocol, with 40 cycles and hybridization at 60 °C. Real-time PCR was performed on a panel of nine differentially expressed genes Bbc3; Efna1; Jun; IkBa; Ninj1; Sesn2; Stc2; Vegfa and Znf184) and three housekeeping genes (β-actin, Gapdh and Mrps14); Differentially expressed genes were selected, for their different average signal intensities in the microarray experiments (sequences of primers in supplemental Table 1).

2.6. Microarray data accessibility

The gene expression profiles reported in this paper have been deposited in the National Center for Biotechnology Information's Gene Expression Omnibus database. The accession number is GSE16026.

2.7. Pathway impact analysis

The lists of differentially expressed genes for the tested contrasts ("TNFα vs. Control", "Heteronemin vs. Control" and the interaction effect between heteronemin and TNFα) were analyzed for impacted KEGG pathways [28] by means of the Pathway Express software [29]. This tool is based on a statistical model taking into account the number of regulated genes in a pathway and furthermore if the observed changes are biologically meaningful.

An impact factor and a related FDR value were computed for every pathway. The impact factor takes into account the fold changes of the regulated genes, the overrepresentation of the group of regulated genes in a given pathway as well as the structural topology of the analyzed pathway [29].

A statistical significance threshold (FDR <0.25) was applied to detect impacted pathways. Only pathways below the significance cut-off for at least one contrast ("TNFα vs. Control", "Heteronemin vs. TNFα" or the interaction effect between heteronemin and TNFα) will be shown.

2.8. Gene Ontology Biological Process enrichment analysis

The different gene lists of up- and down-regulated genes were analyzed for enrichment of biological processes by using the BioConductor package Gostats [30]. Conditional overrepresentation analysis for Gene Ontology (GO) Biological Processes (BP) [31] for the positive and negative gene lists over the three contrasts, including "TNFα vs. Control", "Heteronemin vs. TNFα" and the interaction effect between heteronemin and TNFα, was performed.

All genes, which were tested for differential expression and having at least one annotated GO BP term, were included in the gene universe for GO BP conditional overrepresentation analysis. Only GO BP terms with at least 10 and less than annotated 1000 genes are shown in the resulting tables to avoid to specific or unspecific GO terms.

A statistical significance threshold (*p*-value <0.05) was applied to detect enriched biological processes.

2.9. Enrichment analysis for in silico predicted transcription factor binding site motifs

Promoters of the differentially regulated genes were screened for enriched TFBS motifs using the Clover software [32]. Promoter sequences, 1000 base pairs upstream and 200 base pairs downstream of the transcriptional start site, were retrieved from the "Database of Transcriptional Start Sites" (DBTSS) version 6 [33,34] and scanned for TFBS motifs using the Clover software and the TransFac 2008.4 position weight matrix (PWM) library [35]. Only high quality PWMs related to human transcription factors were used for *in silico* screening.

Clover allows to detect enriched transcription factor binding site (TFBS) motifs by comparing a positive promoter sequence set representing induced or repressed genes in the considered microarray experiment against a set of promoters of not regulated genes (the negative promoter set). As positive promoter set, the promoter sequences for the induced or repressed genes in the different gene lists were used. As negative promoter sequence set, promoters for all genes with related spots (a) which show a fold change less than 1.1 over all contrasts tested, (b) which have an average signal intensity above the lowest signal intensity detected for the significantly regulated spots and (c) for which no other spots related to the corresponding Gene ID were detected as significant over all contrasts, were included.

A statistical significance threshold (*p*-value ≤ 0.01) was applied to detect overrepresented TFBS motifs.

2.10. Electrophoretic mobility shift assay (EMSA)

K562 cells were resuspended in growth medium (RPMI/FCS 0.1%) to a final concentration of 10^6 cells/ml and treated for 2 h with or without heteronemin. The cells were then challenged with

20 ng/ml TNFα for 6 h. Nuclear extracts were prepared as described and stored at −80 °C. The oligonucleotide NF-kappaBc (consensus NF-κB site 50-AGTTGAGGGGACTTTCCCAGGC-30; Eurogentec) and its complementary sequence were used as probe. The probe was hybridized and labeled with [γ-32P] ATP (MP-Biomedicals, Illkirsch, France) and EMSA were performed as published before [36]. Briefly, 10 μg of nuclear extract was incubated in binding buffer with the [γ-32P] ATP labeled probe for 20 min. The DNA–protein complexes were analyzed by electrophoresis on a 5% native polyacrylamide gel and visualized by autoradiography. In immunodepletion experiments, nuclear extracts and labeled probes were incubated on ice for 30 min prior to a 30 min incubation with 2 μg of anti-p50 or anti-p65 antibodies (Santa Cruz Biotechnology, Boechout, Belgium).

2.11. Transient transfection and luciferase reporter gene assay

Transient transfections of K562 cells were performed as previously described [36]. Briefly, 5 μg of luciferase reporter gene construct containing five repeats of a consensus NF-κB site (Stratagene, Huissen, Netherlands) and 5 μg Renilla luciferase plasmid (Promega, Leiden, Netherlands) was used for each pulse. Following electroporation, the cells were resuspended in growth medium (RPMI/FCS 10%) and incubated at 37 °C and 5% CO_2. 20 h after transfection, the cells were harvested and resuspended in growth medium (RPMI/FCS 0.1%) to a final concentration of 10^6 cells/ml and treated for 2 h with or without heteronemin. The cells were then challenged with 20 ng/ml TNFα for 6 h. 75 μl Dual-Glo™ Luciferase Reagent (Promega) were added to the cells for a 10 min incubation at 22 °C before luciferase activity was measured. Then, 75 μl Dual-Glo™ Stop and Glo1 Reagent (Promega) were added for 10 min at 22 °C in order to assay Renilla activity. Luciferase and Renilla (Promega) activities were measured using an Orion microplate luminometer (Berthold, Pforzheim, Germany) by integrating light emission for 10 s. The results are expressed as a ratio of arbitrary units of firefly luciferase activity normalized to Renilla luciferase activity.

2.12. IKK kinase activity

The K-LISA IKKβ Inhibitor Screening kit from Calbiochem was used for the measurement of the kinase activity. IKK-2 Inhibitor IV ([5-(*p*-fluorophenyl)-2-ureido]thiophene-3-carboxamide) (Calbiochem, San Diego, CA)) was used as a positive control. The assay was performed as indicated in the manufacture's protocol. The absorbance at 450 nm (with a reference wave length at 590 nm) was read using a SpectraCount UV-spectrometer (Packard, Groningen, Netherlands).

2.13. Proteasome inhibition activity

The Proteasome-Glo™ Chymotrypsin-Like Cell-Based Assay (Promega) was used in addition to the Trypsin-Like and Caspase-Like Assays to evaluate the three major proteolytic activities. Epoxomycin (at 5 μM) (Sigma, Bornem, Belgium) was used as positive control. The assays were performed as indicated in the manufacture's protocol. Briefly, K562 cells (at a concentration of 10^6 cells/ml in 0.1% FCS medium) were treated with indicated concentrations of NLE. After an incubation period of 8 h, 25×10^3 cells per well were mixed with 25 μl of the recombined cell-based reagent. After vigorous shaking (for 2 min) and an additional incubation period of 10 min at room temperature the luminescence was measured on a luminometer (Berthold). A viability assay, using the CellTiter-Glo® Luminescent Cell Viability Assay Kit from Promega, was performed in parallel to normalize the proteasome activity to the number of viable cells.

2.14. Cell viability assessment

The percentage of cell death after incubation with the test compounds was determined using the CellTiter-Glo® Luminescent Cell Viability Assay Kit (Promega). Assays were performed according to the manufacturer's instructions. Briefly, the assay determines the number of viable cells, based on the quantification of ATP, as indicator of metabolic activity, using the luciferase catalysis of luciferin to oxyluciferin and light in the presence of Mg^{2+}, ATP and oxygen. Lyophilized enzyme/substrate mixture was reconstituted with the provided buffer. Then, an equal volume of the reaction buffer was added to the medium containing K562 cells (untreated or treated with heteronemin at the indicated times). The mixture was shaken on a rocking platform for 2 min, and then incubated for 10 min in the dark at RT. The luminescence signal, proportional to the amount of ATP present, was quantified by using an Orion microplate luminometer, and converted in number of viable cells according to the manufacturer's instructions. Data were normalized to the control and reported as percentage of viable cells.

2.15. Analysis of apoptosis

(a) Analysis of nuclear fragmentation. Percentage of apoptotic cells was quantified as the fraction of apoptotic nuclei, as previously described assessed by fluorescence microscopy (Leica-DM IRB microscope, Lecuit, Luxemburg) upon staining with the DNA-specific dye Hoechst 33342 (Sigma) [37]. The fraction of cells with nuclear apoptotic morphology was counted (at least 300 cells in at least three independent fields). The images were analyzed using the Image J software (http://rsb.info.nih.gov/ij/docs/index.html).

(b) Flow cytometric analysis (annexin V-FITC/propidium iodide-staining) of phosphatidylserine exposure. At the indicated times and doses of treatment, K562 cells were assayed for phosphatidylserine exposure, by using the Annexin V-FITC Apoptosis Detection Kit I® (Becton Dickinson Biosciences, Erembodegem, Belgium) according to the manufacturer's instructions. Stained samples were analyzed by FACS (FACS-Calibur, Becton Dickinson, San José, CA, USA). Data were recorded using the CellQuest software (http://www.bdbiosciences.com/features/products) for further analysis.

2.16. Modulation of apoptosis

The caspase inhibitors z-VAD-FMK, caspase-9 inhibitor II, caspase-8 inhibitor I, were purchased from Calbiochem. They were dissolved in DMSO and added at the concentration of 50 μM, 1 h before heteronemin addition.

2.17. Extraction of cellular proteins

After incubation of Jurkat cells with heteronemin at the indicated times, nuclear and cytoplasmic extracts for the analysis of the translocation of the pro-inflammatory factors were prepared according to [36]. Briefly, 10^7 cells per sample were lysed in a hypertonic detergent medium containing protease inhibitor cocktail (Complete®, Roche, Luxembourg). The extraction was performed on ice to avoid protein degradation. Alternatively, to analyze apoptotic parameters, whole cell extracts were prepared using M-PER® (Mammalian Protein Extraction Reagent) (Pierce, Erembodegem, Belgium) according to the manufacturer's instructions. 10^7 cells per sample were washed with PBS and the pellet was resuspended in 400 μl of M-PER® containing a protease inhibitor cocktail (Complete®, Roche, Luxembourg). The suspension was put on a shaker with vertical agitation for 15 min at +4 °C,

followed by a centrifugation at 15,000 × *g* for 15 min at +4 °C for clarification. Afterwards, supernatants were removed and aliquots were stored at −80 °C until use.

2.18. Western blot analysis

Proteins of total extracts were separated by size using sodium dodecyl sulfate polyacrylamide gel electrophoresis (SDS-PAGE) (10%), transferred onto nitrocellulose membranes and blocked with 5% non-fat milk in phosphate buffered saline (PBS)-Tween overnight. Equal loading of samples was controlled using β-actin, or lamin B and α-tubulin for cytosolic and nuclear extracts. Blots were then incubated with the following primary antibodies: anti-β-actin (1:5000, Sigma), anti-caspase-8, anti-caspase-9 and anti-phospho-IκBα (1:1000; Cell Signaling, Leiden, Netherlands), anti-PARP, anti-caspase-3, anti-Bid, anti-IκBα, anti-p65, and anti-p50 (1:1000; Santa Cruz Biotechnology, Boechout, Belgium). All antibodies were diluted in a PBS-Tween solution containing 5% of bovine serum albumin (BSA) or 5% of milk according to the providers' protocols. After incubation with the primary antibodies, membranes were washed with PBS and incubated for 1 h at RT with the corresponding secondary antibodies following manufacturer's instructions (HRP conjugated goat anti-rabbit or goat anti-mouse from Santa Cruz Biotechnology). After washing with PBS-Tween, specific immunoreactive proteins were visualised by autoradiography using the ECL Plus Western Blotting Detection System Kit® (GE Healthcare, Roosendaal, Netherlands).

3. Results

3.1. Heteronemin significantly impacted cell signaling pathways

In order to better understand the biological effects of heteronemin on chronic myeloid K562 cells, microarray experiments were performed as described in Section 2. Pathway Express software was used to identify significantly modulated pathways by giving a particular focus on inflammation, cell death and cell cycle related pathways. Here it is noteworthy that the MAPK pathway is of particular interest, as it is known to be involved in the regulation of a large panel of cellular processes, including the regulation of inflammation and cell death. As can be seen in Table 1 the "MAPK signaling pathway" pathway was significantly impacted considering the list of differentially expressed gene for the "Heteronemin vs. Control" comparison and for the interaction effect between heteronemin and TNFα. Furthermore, the "Cell cycle" and the "Apoptosis" pathway were significantly impacted for the interaction effect between heteronemin and TNFα. Additionally, "Regulation of autophagy" was significantly modulated considering the list of differentially regulated genes comparing heteronemin-treated cells relative to untreated cells. Even though KEGG

Table 1
Statistically significantly impacted KEGG pathways. Pathways with a significant impact factor as computed by Pathway Express software are shown here. "Pathway Name" indicates the corresponding pathway name while "TNFα vs. Control", "Heteronemin vs. Control" and "Interaction Heteronemin:TNFα" gives the corresponding impact factor. Only pathways with an FDR <0.25 for one of the tested contrasts ("TNFα vs. Control", "Heteronemin vs. TNFα" and "Interaction Heteronemin:TNFα") are shown. Impact factors for pathways with a FDR <0.25 are set to boldface.

Pathway name	TNFα vs. Control	Heteronemin vs. Control	Interaction Heteronemin:TNFα
Acute myeloid leukemia	**3.537**	1.433	**0**
Adherens junction	0	1.018	**7.121**
Adipocytokine signaling pathway	**9.204**	4.81	**8.341**
Allograft rejection	0	0	**4.07**
Apoptosis	**9.461**	2.967	**9.627**
Asthma	**6.467**	0	**4.284**
Axon guidance	**4.864**	0	**5.405**
B cell receptor signaling pathway	**9.154**	4.189	**6.942**
Base excision repair	0	0	**3.467**
Bladder cancer	**4.169**	2.726	0
Cell adhesion molecules (CAMs)	**4.072**	1.884	**4.228**
Cell cycle	**3.107**	4.525	**2.682**
Chronic myeloid leukemia	**3.725**	3.108	**5.515**
Colorectal cancer	**3.029**	3.385	0
Complement and coagulation cascades	**5.804**	1.21	0
Cytokine–cytokine receptor interaction	**27.388**	1.77	**8.233**
DNA replication	0	0	**3.411**
Epithelial cell signaling in *Helicobacter pylori* infection	**16.376**	**10.23**	**7.546**
Fc epsilon RI signaling pathway	**4.576**	0	**3.356**
Focal adhesion	**3.652**	3.746	2.215
Graft-versus-host disease	**6.125**	0	**4.043**
Hematopoietic cell lineage	**9.624**	1.118	**3.265**
Jak-STAT signaling pathway	**3.146**	2.799	**5.095**
Leukocyte transendothelial migration	**6.267**	0	**5.218**
MAPK signaling pathway	**8.786**	**5.441**	**8.769**
Maturity onset diabetes of the young	**4.929**	0	0
mTOR signaling pathway	0	**5.784**	0
Neurodegenerative diseases	0	**5.153**	0
Natural killer cell mediated cytotoxicity	**6.057**	0	**7.489**
Nucleotide excision repair	0	0	**3.237**
p53 signaling pathway	**5.473**	**11.302**	**4.674**
Phosphatidylinositol signaling system	0	**28.002**	0
Prostate cancer	**3.595**	**6.659**	2.938
Regulation of autophagy	0	**6.564**	0
Small cell lung cancer	**7.536**	3.714	**6.507**
T cell receptor signaling pathway	**16.301**	3.735	**8.395**
TGF-β signaling pathway	**5.772**	2.141	**7.566**
Toll-like receptor signaling pathway	**19.087**	4.413	**5.147**
Type I diabetes mellitus	**3.31**	0	**3.942**
Type II diabetes mellitus	**5.389**	4.473	**6.814**

pathways are manually curated pathways, they might not encompass all related genes for a considered biological process, like for example cell death or cell cycle. The GO BP ontology allows taking a broader focus on cellular processes even though the GO BP terms take not into account the precise relationships and dependencies between the related genes.

3.2. Technical validation of microarray data by real-time RT-PCR

We assessed the quality of the microarray experiments by quantitative real-time RT-PCR. These experiments were performed on all samples extracted from the three replicates. Only genes that were detected as differentially expressed were taken into consideration for quality assessment purposes by RT-PCR. These genes were selected randomly, among genes presenting different average signal intensities in the microarray experiments. Results of real-time PCR were transposed in *base 2 logarithms* in order to have comparable scales of values. Analysis of the fold changes obtained by microarray and RT-PCR for the selected genes (Table 2) shows a good correlation between the microarray and the RT-PCR platforms (R^2 = 0.7734). This approach allows validating the efficiency of the microarrays experiments performed.

3.3. Heteronemin modulated biological functions

To confirm the previous results and to gain further insights into the biological effects of heteronemin, overrepresentation analysis for GO BP terms was performed. A large number of processes were found to be associated to the lists of up- and down-regulated genes for the different comparisons (supplemental Table 2). By visual inspection we detected a large panel of themes among the enriched GO BP terms in the heteronemin related gene lists, which are related to cell cycle, cell death, the MAPK pathway and the activation cascade for the transcription factor NF-κB (Table 3).

For the ''Heteronemin vs. Control'' comparison, the list of significantly down-regulated genes is associated with different cell death related GO BP terms, including ''anti-apoptosis'', ''regulation of apoptosis'' and ''programmed cell death''. Furthermore, the list of repressed genes is also associated significantly to different cell cycle related GO BP terms, including ''cell division'' and ''regulation of cyclin-dependent protein kinase activity''.

As for the list of repressed genes, the list of significantly induced genes for the ''Heteronemin vs. Control'' comparison shows an enrichment of genes related to cell death, including ''cell death'', ''positive regulation of programmed cell death'', ''apoptosis'', ''induction of apoptosis'', ''caspase activation'', ''regulation of apoptosis'' and ''regulation of caspase activity''. Additionally topics related to cell cycle including ''cell cycle arrest'' and ''cell cycle'' were found to be associated to the induced gene list. Furthermore a significant association of the NF-κB activation cascade related GO term ''regulation of NF-κB import into nucleus'' was found in this gene list.

The results obtained here, by comparing RNA levels of heteronemin-treated relative to untreated K562 cells, suggest a modulatory effect of heteronemin on apoptosis, cell cycle and the NF-κB activation cascade.

For the lists of differentially expressed genes, considering the interaction effect of heteronemin and TNFα, significant associations for the cell death related topics were found with the list of negatively regulated genes, including ''cell death'', ''negative regulation of programmed cell death'', ''anti-apoptosis'', ''induction of apoptosis'', ''regulation of apoptosis'', ''positive regulation of programmed cell death'', ''caspase activation'', ''regulation of caspase activity'', ''apoptosis'', ''DNA damage response, signal transduction resulting in induction of apoptosis'' and ''induction of apoptosis via death domain receptors''. Different GO BP terms which point to an antagonistic effect of heteronemin and TNFα on cell cycle were also detected, including ''interphase of mitotic cell cycle'', ''positive regulation of mitosis'' and ''S phase''. Furthermore MAPK pathway and NF-κB activation cascade related GO terms, including ''positive regulation of JNK cascade'', ''I-κB kinase/NF-κB cascade'' and ''positive regulation of NF-κB transcription factor activity'' were also found among the enriched biological topics in the list of genes showing a negative interaction effect between heteronemin and TNFα. It is noteworthy, that only one gene, TNFα itself is associated with the ''positive regulation of JNK cascade'' term in the considered gene list.

Interestingly, no cell death, cell cycle, MAPK pathway or NF-κB activation pathway related terms were significantly associated to the list of induced genes considering the interaction effect between heteronemin and TNFα.

Considering the lists of induced and repressed genes for the interaction contrast between heteronemin and TNFα and the associated GO BP terms respectively, the results suggest that both molecules have antagonistic effects on biological processes and genes tightly associated to the regulation of cell death, cell cycle and the NF-κB activation cascade.

Altogether, the results obtained previously for pathway impact analysis and GO BP enrichment analysis strongly suggest a modulatory effect of heteronemin on cell death and cell cycle as well as the MAPK pathway and the NF-κB activation cascade.

3.4. Heteronemin regulated inflammation related transcription factors

To uncover transcriptional regulators modulated by heteronemin, overrepresentation analysis for TFBS was performed. A specific aim here was to see if inflammatory response related TFBS were significantly enriched.

Table 2
Correlation between microarrays and real-time PCR data. Results obtained with microarrays were compared to measure of the expression of a panel of nine genes by real-time PCR. The results of real-time PCR are transposed in *base 2 logarithms* in order to have comparable scales of values. The results show a correlation of R^2 = 0.7734.

Gene symbol	Microarray			RT-PCR		
	Heteronemin vs. Control	TNFα vs. Control	Heteronemin +TNFα vs. TNFα	Heteronemin vs. Control	TNFα vs. Control	Heteronemin +TNFα vs. TNFα
BBC3	2.21	0.74	1.54	2.10	0.19	2.15
EFNA1	0.04	1.27	−0.81	0.33	2.13	−1.08
JUN	2.51	1.11	1.80	3.94	0.93	2.98
NFKBIA	1.26	3.10	0.00	0.80	3.18	−0.66
NINJ1	−0.02	1.40	−0.68	−0.32	1.33	−0.86
SESN2	1.43	0.13	1.37	2.55	0.03	2.55
STC2	1.54	0.05	1.50	2.07	−0.14	2.01
VEGFA	0.67	0.02	0.84	1.72	0.08	1.95
ZNF184	0.68	−0.07	0.92	0.87	−0.28	0.77

Table 3
Statistically significantly enriched GO BP terms related to cell cycle, cell death, MAPK pathway and NF-κB activation cascade. Statistically significantly overrepresented GO BP terms (p-value <0.05) related to selected cellular processes (cell cycle, cell death, MAPK pathway and NF-κB activation cascade) are shown for the lists of significantly up- and down-regulated genes considering the comparisons "Heteronemin vs. Control" and "Interaction Heteronemin:TNFα". Column 1 indicates the GO BP term tested for overrepresentation. Column 2 indicates the corresponding p-value. Column 3 indicates the related gene symbols to the enriched GO BP term.

Heteronemin vs. Control		
Negative gene list		
Cell division	1.50E−02	CCND1, CDC26, CKS2, NDE1, SPC25
Anti-apoptosis	1.66E−02	CCL2, DAD1, PRNP, SOCS3
Regulation of cyclin-dependent protein kinase activity	3.09E−02	C13orf15, CKS2
Regulation of apoptosis	4.07E−02	CCL2, DAD1, DYRK2, PRNP, SOCS3, SPN, UTP11L
Programmed cell death	4.86E−02	CCL2, DAD1, DYRK2, PHLDA2, PRNP, SOCS3, SPN, TNFRSF12A, UTP11L
Positive gene list		
Cell cycle arrest	4.24E−07	CDKN1B, DDIT3, GADD45A, HBP1, ING4, JMY, MLL5, PPP1R15A, SESN2
Cell death	2.48E−05	AIFM2, BBC3, BTG1, CASP10, CDKN1B, CEBPB, CEBPG, DDIT3, DDIT4, GADD45A, IHPK2, ING4, JMY, MDM4, NFKBIA, NLRP12, PMAIP1, PPP1R15A, RFFL, SQSTM1, TNFAIP3, TRIB3, VEGFA
Positive regulation of programmed cell death	5.13E−04	AIFM2, BBC3, CASP10, CDKN1B, CEBPB, CEBPG, DDIT3, IHPK2, JMY, PMAIP1
Apoptosis	9.54E−04	DDIT4, GADD45A, ING4, MDM4, NFKBIA, PPP1R15A, RFFL, SQSTM1, TRIB3
Induction of apoptosis	1.72E−03	AIFM2, BBC3, CASP10, CDKN1B, CEBPB, CEBPG, JMY, PMAIP1
Cell cycle	5.22E−03	BOLL, CCNG2, CDKN1B, DDIT3, DUSP1, G0S2, GADD45A, HBP1, ING4, JMY, MDM4, MLL5, PPP1R15A, RGS2, SESN2, TMPRSS11A, TUBB2B
Regulation of NF-κB import into nucleus	8.53E−03	NFKBIA, NLRP12
Caspase activation	8.73E−03	BBC3, NLRP12, PMAIP1
Regulation of apoptosis	1.13E−02	AIFM2, BTG1, CASP10, CDKN1B, CEBPB, CEBPG, DDIT3, IHPK2, JMY, TNFAIP3, VEGFA
Regulation of caspase activity	2.00E−02	BBC3, NLRP12, PMAIP1
Interaction Heteronemin:TNFα		
Negative gene list		
Cell death	1.34E−06	ABL1, BBC3, BCL3, BIRC3, CCL2, IER3, NFKBIA, PTPN6, SGPP1, TNF
Negative regulation of programmed cell death	6.13E−05	BCL3, BIRC3, CCL2, IER3, TNF
Anti-apoptosis	2.23E−04	BIRC3, CCL2, IER3, TNF
Induction of apoptosis	5.78E−04	ABL1, BBC3, BCL3, TNF
Regulation of apoptosis	1.17E−03	ABL1, BCL3, BIRC3, CCL2, IER3
Positive regulation of programmed cell death	1.39E−03	ABL1, BBC3, BCL3, TNF
Caspase activation	2.55E−03	BBC3, TNF
Regulation of caspase activity	4.66E−03	BBC3, TNF
Apoptosis	5.05E−03	NFKBIA, PTPN6, SGPP1
Interphase of mitotic cell cycle	1.04E−02	ABL1, POLE
DNA damage response, signal transduction resulting in induction of apoptosis	1.94E−02	ABL1
Induction of apoptosis via death domain receptors	2.11E−02	TNF
I-κB kinase/NF-κB cascade	2.44E−02	BCL3, TNF
Positive regulation of JNK cascade	2.49E−02	TNF
Positive regulation of mitosis	3.43E−02	TNF
S phase	3.80E−02	ABL1
Positive regulation of NF-κB transcription factor activity	4.36E−02	TNF
Positive gene list		
/	/	/

The lists of differentially expressed genes were compared to a reference list based on the *in silico* predictions of TFBS using the high quality set of PWMs related to human transcription factors from TransFac 2008.4. A complete listing of statistically significantly enriched TFBS motifs can be found in supplemental Table 3.

As shown in Table 4 significant associations between the negative gene list for the "Interaction Heteronemin:TNFα" contrast and a large panel of NF-κB specific PWMs were detected, including V$CREL_01, V$NFKAPPAB_01, V$NFKAPPAB65_01, V$NFKB_C, V$NFKB_Q6 and V$NFKB_Q6_01. Additionally, as can be seen in supplemental Table 3 no enriched NF-κB related PWMs were detected for the list of up-regulated genes considering the "Interaction Heteronemin:TNFα" contrast and for the lists of up- and down-regulated genes when comparing heteronemin-treated K562 cells to untreated cells, while for the "TNFα vs. Control" comparison a significant association of NF-κB specific PWMs were found with the list of induced genes, including V$CREL_01, V$NFKAPPAB_01, V$NFKAPPAB50_01, V$NFKAPPAB65_01, V$NFKB_C, V$NFKB_Q6 and V$NFKB_Q6_01.

These results together with the results obtained for the enrichment analysis of GO BP terms, suggest an inhibition of the activation cascade for the transcription factor NF-κB following TNFα-mediated activation of this factor in K562 cells which results in a downstream transcriptional repression of its direct target genes.

3.5. Heteronemin significantly inhibited TNFα-induced NF-κB pathway activation

The use of high-throughput profiling to identify the changes in gene expression induced by heteronemin in chronic myeloid leukemia K562 cells revealed a potential effect on inflammation and cell death.

Table 4
Statistically significantly enriched inflammatory response related TFBS. Statistically significantly overrepresented TFBS motif (p-value ≤ 0.01), which are related to inflammatory response specific transcription factors, are shown for the lists of repressed genes considering the interaction effect between heteronemin and TNFα. "Matrix Name" indicates the name of the PWM used for scanning the promoter sequences for TFBS. "Transcription factor" indicates the name of the transcription factor or the family of transcription factors associated with the corresponding PWM.

Interaction Heteronemin:TNFα		
	Matrix name	Transcription factor
Negative gene list	V$CREL_01	c-Rel
	V$NFKAPPAB_01	NF-κB
	V$NFKAPPAB65_01	NF-κB (p65)
	V$NFKB_C	NF-κB
	V$NFKB_Q6	NF-κB
	V$NFKB_Q6_01	NF-κB

First, we investigated the potential ability of heteronemin to modulate inflammation by analyzing its impact on a pro-inflammatory pathway model represented by TNFα-induced transcriptional activity of NF-κB. To this purpose, as first approach, we used a luciferase reporter gene assay.

Transfected cells were pre-treated for 2 h with different concentrations of heteronemin (Fig. 2A) and challenged for 6 h with 20 ng/ml of TNFα. The results showed that heteronemin reduced TNFα-induced NF-κB activation in a dose-dependent manner (Fig. 2A), starting from a concentration of 4.0 μM.

To confirm the inhibitory effects of heteronemin on the TNFα-induced NF-κB pathway, we investigated any ability of heteronemin to interfere with the NF-κB-DNA binding by performing an EMSA assay. Fig. 2B shows that heteronemin inhibited TNFα-induced NF-κB-DNA binding, thus achieving a complete inhibition starting from 4.0 μM in K562 cells. Incubation with p50 or p65 antibodies led to the identification of the p50/p65 dimer. Competition experiments with unlabeled NF-κB probes resulted in a complete disappearance of the band. Similar results are achieved for Jurkat cell line (Fig. 2C).

As activation of NF-κB is initiated by degradation of the natural inhibitor IκBα, we next assessed integrity of IκBα as well as the translocation of p50 and p65 to the nucleus by Western blot analysis. To this purpose, we used Jurkat cells, a system model previously deeply investigated in parallel to K562 in our lab for NF-κB studies [20,38]. First of all, we confirmed that heteronemin was able to inhibit TNFα-induced NF-κB activation in a dose-dependent manner by luciferase assay (Fig. 3A). Next, Jurkat cells were pre-treated for 2 h with 5.6 μM heteronemin, then challenged with 20 ng/ml TNFα and the translocation into the nucleus of p65 and p50 together with the analysis of IκBα degradation were analyzed by WB (Fig. 3B). In TNFα-stimulated cells, IκBα degradation occurs starting from 15 min; concomitantly, the translocation to the nucleus of NF-κB subunits p50 and p65 was observed (Fig. 3B, left). Heteronemin (Fig. 3B, right) completely prevented TNFα-induced degradation of IκBα and the subsequent translocation of p50 and p65 to the nucleus. Furthermore, use of phospho-IκBα antibody indicated that TNFα-stimulated the phosphorylation of IκBα with a maximum at 10 min (Fig. 3C, left). Heteronemin (Fig. 3C, right) strongly attenuates the IκBα phosphorylation.

As degradation of IκBα depend either on IKK or proteasome activity, we then determined the inhibition potential of heteronemin on IKKβ activity and the proteasome activity using two assays (Fig. 4). First, the level of IKKβ activity in presence of heteronemin was monitored using an IκBα substrate and IKKβ His·Tag®. We showed that heteronemin did not significantly inhibit IKKβ activity at a concentration of 11.2 μM (Fig. 4A), a much higher concentration in contrast to the examined range. Next, we evaluated the protease inhibition activity of heteronemin on three different proteolytic sites (chymotrypsin-, trypsin- and caspase-like) of the 26S proteasome until the representative concentration value of 2.8 μM. Above this value, a plateau-effect was observed which led us to the determination of the proteasome inhibition activity with doses lower than 2.8 μM (Fig. 4B). The results indicated that 0.5 μM of heteronemin inhibited 55% of chymotrypsin- and trypsin-like proteolytic activity (IC_{50} = 0.4 μM for both) and 30% of caspase-like activity ($IC_{50} > 2.8$ μM). Hence, heteronemin inhibited significantly proteasome activity. Altogether, these results indicate an ability of heteronemin to inhibit the activation of NF-κB pathway.

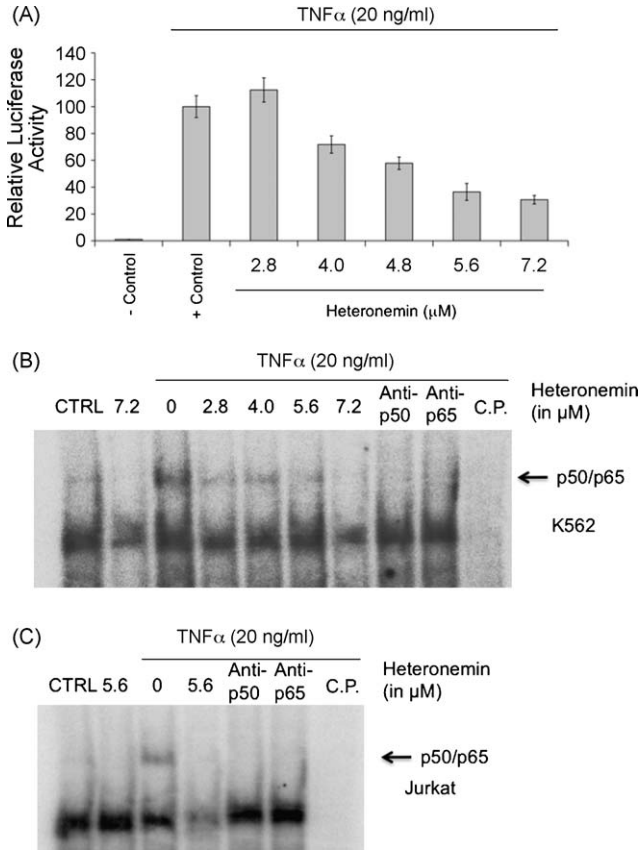

Fig. 2. Inhibition of TNFα-induced NF-κB activation by heteronemin. K562 cells were pre-treated with heteronemin at various concentrations of 2.8–7.2 μM and incubated for 2 h, followed by TNFα addition (at 20 ng/ml) and an additional incubation period of 6 h. (A) Effect of heteronemin on the inhibition of TNFα-induced NF-κB activation assessed by a Dual-Glo™ Luciferase assay system on a K562 cell line. The results of the luciferase NF-κB reporter gene assay represented the ratio of the measured luminescence of the firefly luciferase vector divided by the measured luminescence of the Renilla plasmid. An untreated cell solution was the negative control, positive control was a cell solution treated with TNFα only. Results were presented as mean ± SD of eight individual measurements. Experiments were performed in triplicate, SD was less than 10% and typical data are shown. (B) Effect of heteronemin on the binding affinity of NF-κB assessed by an EMSA on K562 cells. The DNA binding affinity was determined by an incubation of the nuclear cell extract (10 μg), prepared according to Muller and co-workers [51], with a labeled oligonucleotide probe containing the NF-κB binding site C-κB, with the indicated antibodies and an unlabeled NF-κB probe (C.P.). The data shown here were representative for three independent experiments with similar results. (C) Effect of heteronemin on the binding affinity of NF-κB assessed by an EMSA on Jurkat cell line. One representative of three independent experiments is shown.

3.6. Heteronemin induced caspase-dependent apoptosis in K562 cells

Next, we evaluated any impact of heteronemin on cell viability. K562 cells were treated with different concentrations of hetero-

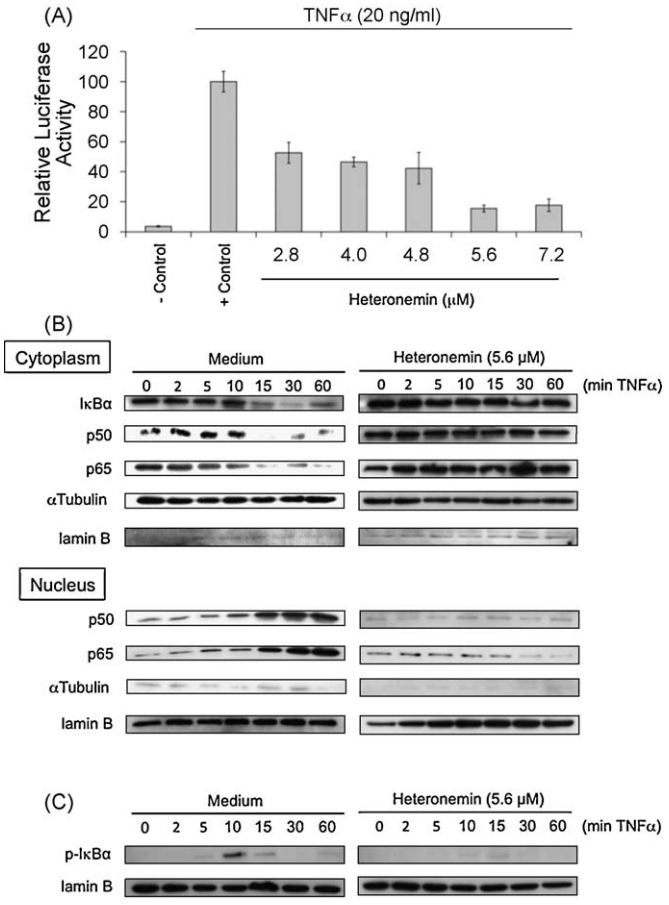

Fig. 3. Effect of heteronemin on the degradation of IκBα and translocation of p65 and p50 to the nucleus. (A) Effect of heteronemin on the TNFα-induced NF-κB activation assessed by a Dual-Glo™ Luciferase assay system on Jurkat cells. The results and experimental design of the luciferase NF-κB reporter gene assay represented here is similar to Fig. 1A. (B) Jurkat cells were incubated with heteronemin (at 5.6 μM) for 2 h, followed by a TNFα (20 ng/ml) treatment for the indicated time periods. Cytoplasmic and nuclear extracts were prepared, fractionated on a 10% SDS-PAGE gel, transferred to a membrane and then tested for IκBα, p50, p65 (cytosolic) or p50 and p65 (nuclear). Equality of protein loading and purity of nuclear/cytosolic extracts was checked by lamin B and α-tubulin Western blots. The data shown here were representative for three independent experiments with similar results. (C) Effect of heteronemin on phosphorylation of IκBα by TNFα. A pre-treatment of heteronemin (at 5.6 μM) for 2 h is followed by a TNFα (20 ng/ml) treatment for the indicated time periods. Cytoplasmic extract is tested for phospho-IκBα. Equality of protein loading and purity of nuclear/cytosolic extracts was checked by lamin B Western blots. The data shown here were representative for three independent experiments with similar results.

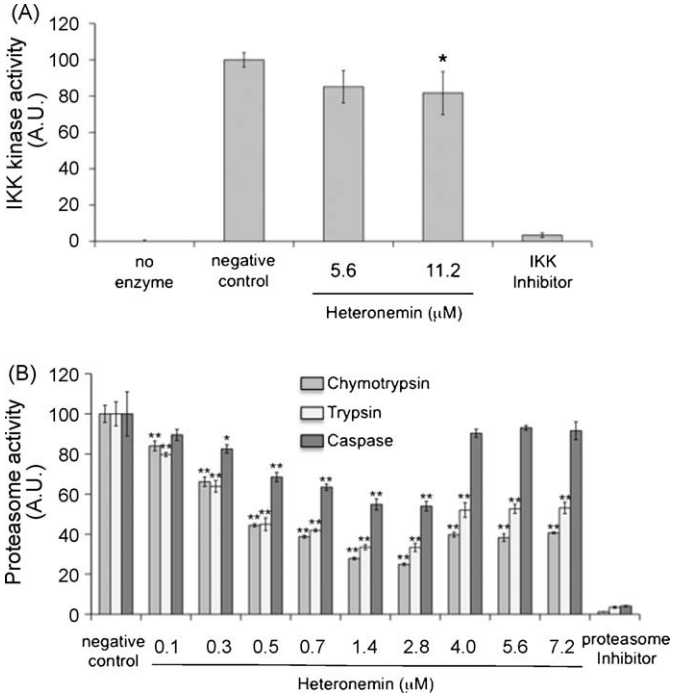

Fig. 4. Effect of heteronemin on the activity of IKK and proteasome activity. (A) Effect of heteronemin at the indicated concentrations on the kinase activity of IKKβ for an incubation period of 30 min at 30 °C. "no enzyme" was performed without IKKβ and "negative control" was determined without any test compound but in the presence of IKKβ. IKK-2 Inhibitor IV (Calbiochem) was used at the recommended concentration of 1 μM. Results are shown as representative mean ± SD of three individual measurements. Asterisk (*) represents $p < 0.05$ compared to the negative control. (B) Effect of heteronemin at the indicated concentrations on the proteolytic activity of the 26S proteasome in K562 cells. Results are shown as a ratio of the luminescence of the firefly luciferase activity of the proteasome kit (using a Proteasome-Glo™ Chymotrypsin-Like Cell-Based Assay from Promega) over the firefly luciferase activity of the viability kit (CellTiter-Glo® Luminescent Cell Viability Assay Kit from Promega) to get a standardized result associated to the number of viable cells. "Negative Control" refers to a control with no test compound. 5 μM of the known proteasome inhibitor epoxomycin was used as positive control. Results are shown as representative mean ± SD of three individual experiments. Asterisks (*) and (**) represent $p < 0.05$ or $p < 0.01$, respectively, compared to the negative control.

nemin for 8 h. Then, cell viability was assessed by quantifying the percentage of metabolically active cells (see Section 2). As reported in Fig. 5A, heteronemin induced cell death in a dose-dependent manner in a range between 24 ± 5% and 80 ± 1%.

In order to understand whether the reduction in cell viability was due to apoptosis, we tested treated cells for the appearance of typical nuclear apoptotic morphology, by staining the nuclei with Hoechst and fluorescence microscope analysis. Nuclei of cells treated with heteronemin underwent a typical apoptotic nuclear fragmentation (Fig. 5B). Fig. 5C shows the corresponding kinetic analysis of apoptosis induction upon heteronemin challenge, as estimated by counting the percentage of cells respect the total with fragmented nuclei. The values after 8 h of treatment confirmed results from the cell viability test, thus indicating that the effects on the ATP quantification were exclusively due to an impact on cell death and not to additional effects on cell metabolism. The analysis of phosphatidylserine exposure confirmed that the cell death occurred via apoptosis induction (Fig. 5D).

Next, we evaluated whether heteronemin triggered a caspase-dependent apoptotic pathway. To this purpose, the concentration of 5.6 μM was chosen for further investigations. PARP, the known caspase-3 target, was cleaved as early as 4 h of treatment (Fig. 6A, top). In agreement with these results, caspase-3 was activated in a time-dependent manner reaching the maximum of cleavage between 6 and 8 h (Fig. 6A, top), as expected by fluorescence microscope and FACS analysis (Fig. 5B–D). This was preceded by the cleavage of pro-caspase-9 and -8, two crucial players of the intrinsic and extrinsic apoptotic pathway, respectively, operating upstream to caspase-3 [14] (Fig. 6A, bottom). Since the simultaneous cleavage of caspase-8 and -9 might be due to a cross-talk between the two apoptotic pathways via truncation of Bid [15], we investigated such a possible interference. To this purpose, we monitored the appearance of the truncated form of Bid by WB analysis (Fig. 6B). We found that Bid was truncated quite early, starting from 4 h of treatment, thus indicating the possibility of caspase-9 activation via caspase-8.

So far, we ascertained the cleavage/activation of the most implicated caspases in apoptosis [14]. Next, we evaluated whether this activation was really required for the effect on apoptosis, by using specific caspase inhibitors. As shown in Fig. 6C, the pan-inhibitor z-VAD efficiently prevented the pro-apoptogenic activity of heteronemin; specific caspase-9 and -8 inhibitors counteracted apoptosis at a similar level and more strongly when co-added

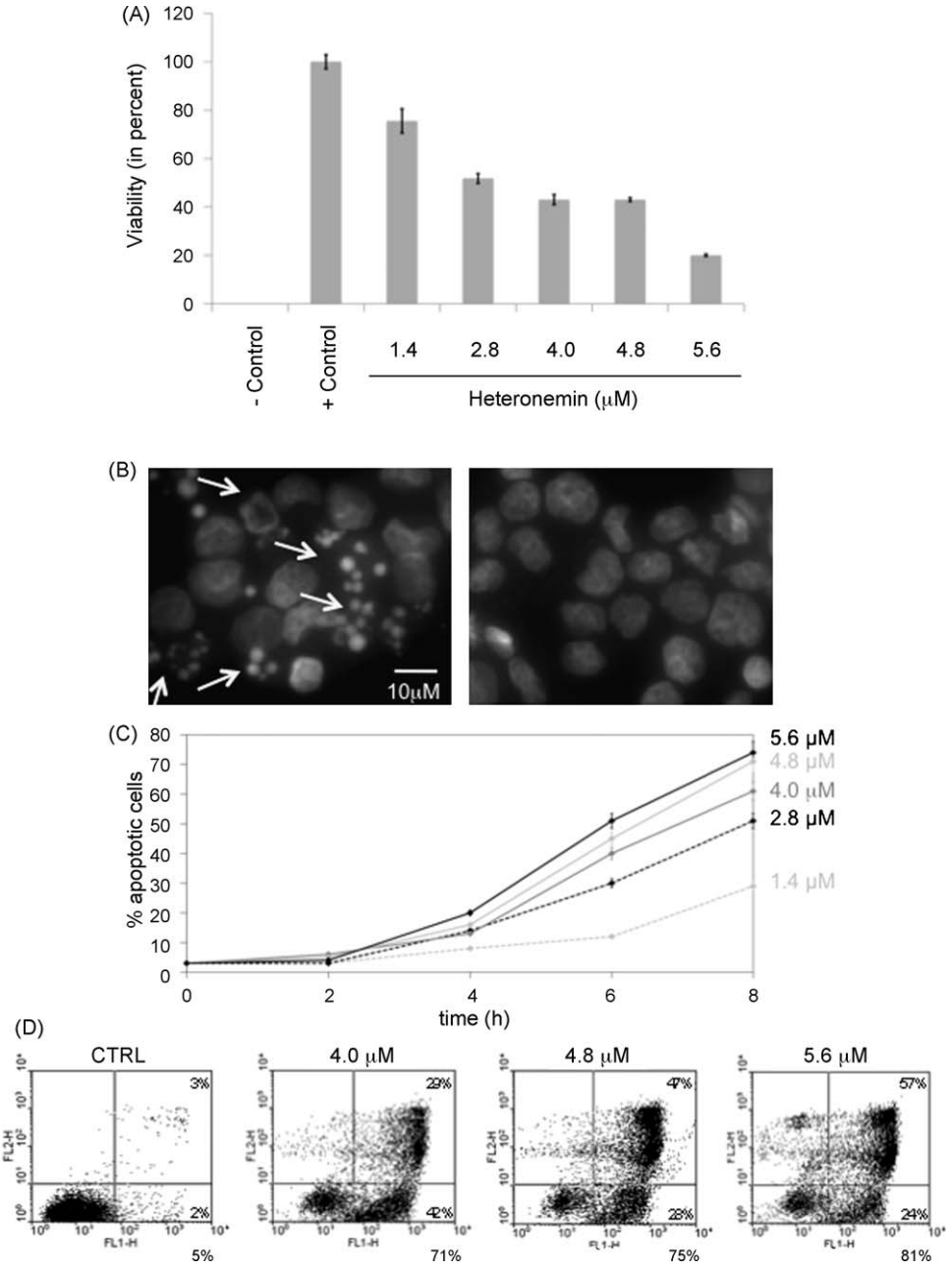

Fig. 5. Heteronemin affects cell viability via apoptosis induction. (A) Luciferase assay to assess the effect of heteronemin on cell viability of K562 cells. Cells were treated 8 h with 5.6 μM heteronemin. Then, the number of viable cells was determined as the number of metabolically active cells (ATP quantification). Data are depicted as mean ± SD (n = 3). (B) Representative image of K562 cells stained with Hoechst to detect nuclear morphology [37], untreated (right panel) vs. treated with 5.6 μM heteronemin for 8 h (left panel), the latter presenting typical fragmented apoptotic nuclei (white arrows). (C) Kinetic analysis of apoptosis induced by heteronemin, evaluated as the fraction of cells with apoptotic nuclei stained with Hoechst. The data are the mean of n = 3 independent experiments ± SD. (D) Detection of apoptotic cells after annexin V-FITC/propidium iodide (PI)-staining by FACS. The lower right quadrant of the plot indicates early apoptotic cells that are only positive for annexin V. One of three independent experiments with similar results is shown.

(Fig. 6C), thus indicating the relevance of both caspases in the resulting apoptosis. Altogether, these results indicated that heteronemin triggers caspase-dependent apoptosis in K562 cells, involving the activation of both caspase-8 and-9.

K562 cells were described to be resistant to apoptosis induced by TNFα [39]. Finally, we wanted to assess whether heteronemin was also able to sensitize K562 cells to the apoptogenic effect of TNFα. To this purpose, K562 cells were pre-treated with heteronemin at a concentration of 0.7 μM, sufficient to affect the NF-κB pathway (Fig. 2B) but only mildly the cell viability (data not shown), and then challenged with TNFα. Fig. 7 shows the analysis of apoptosis estimated by FACS in terms of phosphatidylserine exposure. The results showed a percentage of apoptotic cells treated with both TNFα and heteronemin that was higher compared to cell death achieved by single treatments, thus indicating a synergistic rather than an additive effect of the co-treatment. This indicates that low concentrations of heteronemin sensitize K562 cells to TNFα-induced apoptosis and implies that the modulation of NF-κB pathway might be implicated.

4. Discussion

In this study, we show by using a DNA microarray functional profiling approach that the spongean sesterterpene heteronemin

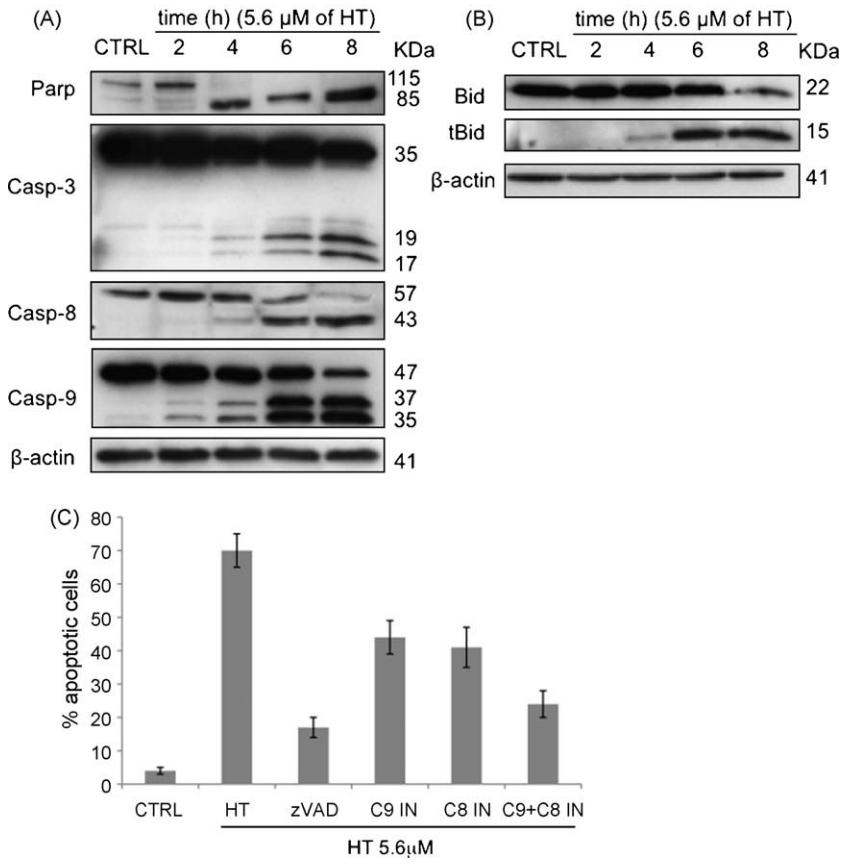

Fig. 6. Heteronemin triggers a caspase-dependent apoptosis. (A) Analysis of the cleavage of pro-caspases -3, -8, -9 and PARP by Western blot. Cells were incubated with the test compound and the cleavage of the protein after 2, 4, 6 and 8 h was investigated in comparison with a non-treated sample (CTRL). Actin was used as a control of constant protein loading of samples. (B) Assessment of the activation of Bid by heteronemin in K562 cells by Western blot analysis. One of three independent experiments is shown in (A) and (B). (C) Analysis of the impact of caspases inhibitors on the ability of heteronemin to trigger apoptosis. K562 cells were pre-treated 1 h before with the pan-inhibitor z-VAD, caspase-9, -8, -9 + -8 inhibitors, used at the concentration of 50 μM. The data are the mean of three independent experiments ± SD.

modulates on a transcriptional level several important pathways and processes related to cell proliferation and survival, including cell cycle arrest, apoptosis, autophagy, the MAPK signaling pathway and the inhibition of the NF-κB activation cascade. Focusing our attention on the potential modulation of inflammation and cell death, we confirmed by in vitro studies that heteronemin is able to exert an anti-inflammatory action. The stimulation of chronic myeloid leukemia K562 cells with the pro-inflammatory cytokine TNFα was our model of investigation to mimic a pro-inflammatory condition involving NF-κB activation.

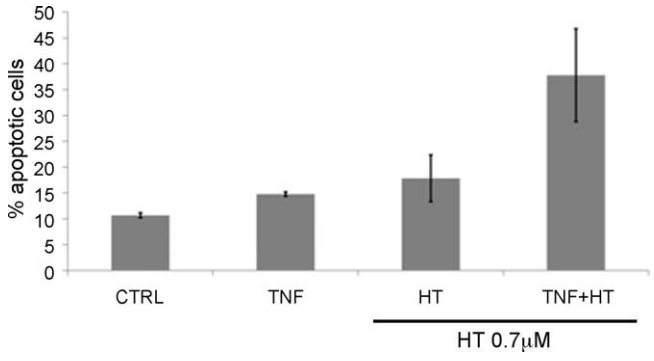

Fig. 7. Heteronemin sensitizes K562 cells to TNFα-induced apoptosis. Effect of heteronemin on TNFα-induced apoptosis. K562 cells were pre-treated 2 h with 0.7 mM of heteronemin and then incubated for 8 h with TNFα (20 ng/ml). The data, as assessed by annexin V-FITC/PI staining and FACS analysis, are the mean of three independent experiments ± SD.

Heteronemin completely prevents TNFα-induced NF-κB activation, as indicated by the complete prevention of both IκBα degradation and phosphorylation through inhibition of the 26S proteasome and the consequent p65 and p50 nuclear translocation. In addition, we show that heteronemin deeply affects cell viability by triggering caspase-dependent apoptosis. Related to the effects on cell death, the compound was able to activate both initiator caspases -8 and -9, which are implicated in the extrinsic and intrinsic apoptotic pathway, respectively [14]. The strong and early truncation of Bid (detectable from 4 h of treatment), known to occur downstream to caspase-8 activation [15], indicates the existence of a cross-talk between the two apoptotic pathways and suggests that the activation of the extrinsic caspase-8-mediated apoptotic pathway might play a crucial and early role in the induction of apoptosis by heteronemin.

Considerable work has been published on the anti-cancer and anti-inflammatory effects of marine natural products. Several of these studies have been focused on the anti-inflammatory and antitumor effects of spongean sesterterpenes in human cell models. Thus, modulatory effects on apoptosis, cell cycle and the NF-κB activation cascade have already been described for different sesterterpenes, including Cyclolinteinone, Ircinin-1 and Strobilin–felixinin. Cyclolinteinone, which is extracted from sponge *Cacospongia linteiformis* is able to block lipopolysaccharide-induced NF-κB activation in a macrophage cell line [40]. The sesterterpene Ircinin-1 has been shown to induce G1 cell cycle arrest and apoptosis in a human melanoma cell line [41], while Strobilin–felixinin exerts its molecular effects by cell cycle arrest in S phase and inhibition of topoisomerase I and polymerase α-

primase [42]. The pentacyclic core unit of heteronemin makes this molecule less flexible than the linear counter-parts. This rigid core might explain the specific bioactivity of heteronemin. In addition, the latter does not possess a lactone unit leading to Michael-addition reaction of nucleophilic cysteine sulfhydryl groups of the p65 monomer in the case of sesquiterpenes [43]. Moreover, it has to be noted that Michael acceptors are normally rejected as possible drug candidates as other proteins and glutathione might also interfere with a lactone group [43,44].

So far, heteronemin has been characterized for its potentially anti-tubercular properties [45]. To our knowledge, this is the first time that anti-inflammatory as well as pro-apoptogenic activities have been described. In this context, this is the first study using a systems biology approach based on DNA microarrays and integrative data mining techniques for the functional profiling of a marine natural compound as a potential anti-cancer therapeutic.

Interestingly, heteronemin is able to massively induce apoptosis in a cell model well known to be strongly resistant to anti-cancer treatments acting via induction of apoptosis. Since the NF-κB pathway is constitutively activated in K562 cells via Bcr-Abl and may be further stimulated in response to apoptogenic agents as part of a pro-survival strategy [46], at our level of investigation, we cannot exclude that the effects exerted by heteronemin on NF-κB, may directly play a role in promoting/favouring the triggering of apoptosis. Interestingly, K562 cells that are resistant to the apoptogenic effect of TNFα [39], become sensitized when co-treated with low concentrations of heteronemin able to inhibit the NF-κB pathway but without cytotoxicity. Results imply that the modulation of the NF-κB pathway might be implicated in cellular resistance.

Alternatively, the modulation of the NF-κB and apoptosis pathways may represent two faces of the same coin, conceivably being the processes independent but regulated by a common factor modulated by heteronemin. Interestingly, our functional profiling studies identify MAPK pathway as a target of heteronemin. The MAPK pathway is known to be an important regulator of NF-κB transcription factor [47]; moreover, it is also implicated in the regulation and induction of apoptosis. These pieces of evidence suggest an implication for the MAPK signaling pathway as a possible mediator for both anti-inflammatory and pro-apoptogenic properties of heteronemin and prompt us to investigate in the future the effective role played by MAPKs in the biological effects of heteronemin.

The regulation of protein degradation is deeply implicated in cancer development, thus the proteasome became a major target in cancer therapy. Bortezomib (VELCADE®) and salinosporamide A (NPI-0052®), two novel proteasome inhibitors validated this therapeutic approach. The natural γ-lactam-β-lactone NPI-0052 is in clinical trials, whereas VELCADE has been approved by FDA for the treatment of multiple myeloma. The response rate of the latter is 35%, but its use is related to toxicity and drug resistance development [48–50]. Thus the discovery of novel natural proteasome inhibitors could open a new point of view in this promising cancer research field. As in the case of NPI-0052, heteronemin strongly inhibits all three proteolytic activities; thereby a high level of proteolysis is induced.

In conclusion, in this study we delineated on a human chronic myeloid cell model novel anti-inflammatory and apoptogenic properties for the spongean sesterterpene heteronemin, as assessed by DNA microarray profiling analysis integrated with in vitro studies. This makes this compound eligible for further mechanistic studies as a potential anti-inflammatory and anti-cancer agent.

Acknowledgments

The authors thank E. Henry and J. Ghelfi for technical assistance. This work was supported by Télévie, the "Fondation de Recherche Cancer et Sang" and "Recherches Scientifiques Luxembourg" asbl. MS, CC, SE, SC were supported by Télévie grants (Fonds National de la Recherche Scientifique, Belgium). The authors thank "Een Häerz fir Kriibskrank Kanner" association and the Action Lions "Vaincre le Cancer" for generous support. We wish to thank the NCI Open Repository Program for providing the crude extract of *Hyrtios* sp. MJ is the recipient of a BBSRC Research Development Fellowship.

Appendix A. Supplementary data

Supplementary data associated with this article can be found, in the online version, at doi:10.1016/j.bcp.2009.09.027.

References

[1] Newman DJ, Cragg GM. Natural products as sources of new drugs over the last 25 years. J Nat Prod 2007;70:461–77.
[2] Donia M, Hamann MT. Marine natural products and their potential applications as anti-infective agents. Lancet Infect Dis 2003;3:338–48.
[3] Blunt JW, Copp BR, Hu WP, Munro MH, Northcote PT, Prinsep MR. Marine natural products. Nat Prod Rep 2008;25:35–94.
[4] Molinski TF, Dalisay DS, Lievens SL, Saludes JP. Drug development from marine natural products. Nat Rev Drug Discov 2009;8:69–85.
[5] Gilmore TD. Introduction to NF-kappaB: players, pathways, perspectives. Oncogene 2006;25:6680–4.
[6] Senftleben U, Karin M. The IKK/NF-kappaB pathway. Crit Care Med 2002;30:S18–26.
[7] Karin M, Greten FR. NF-kappaB: linking inflammation and immunity to cancer development and progression. Nat Rev Immunol 2005;5:749–59.
[8] Coussens LM, Werb Z. Inflammation and cancer. Nature 2002;420:860–7.
[9] Perona R, Sanchez-Perez I. Signalling pathways involved in clinical responses to chemotherapy. Clin Transl Oncol 2007;9:625–33.
[10] Reuter S, Eifes S, Dicato M, Aggarwal BB, Diederich M. Modulation of anti-apoptotic and survival pathways by curcumin as a strategy to induce apoptosis in cancer cells. Biochem Pharmacol 2008;76:1340–51.
[11] Ahn KS, Sethi G, Aggarwal BB. Reversal of chemoresistance and enhancement of apoptosis by statins through down-regulation of the NF-kappaB pathway. Biochem Pharmacol 2008;75:907–13.
[12] Baud V, Karin M. Is NF-kappaB a good target for cancer therapy? Hopes and pitfalls. Nat Rev Drug Discov 2009;8:33–40.
[13] Coppola S, Ghibelli L. GSH extrusion and and the mitochondrial pathway of apoptotic signalling. Biochem Soc Trans 2000;28:56–61.
[14] Fulda S, Debatin KM. Extrinsic versus intrinsic apoptosis pathways in anticancer chemotherapy. Oncogene 2006;25:4798–811.
[15] Henshall DC, Bonislawski DP, Skradski SL, Lan JQ, Meller R, Simon RP. Cleavage of bid may amplify caspase-8-induced neuronal death following focally evoked limbic seizures. Neurobiol Dis 2001;8:568–80.
[16] Cha YJ, Kim HS, Rhim H, Kim BE, Jeong SW, Kim IK. Activation of caspase-8 in 3-deazaadenosine-induced apoptosis of U-937 cells occurs downstream of caspase-3 and caspase-9 without Fas receptor-ligand interaction. Exp Mol Med 2001;33:284–92.
[17] Schoch C, Kohlmann A, Schnittger S, Brors B, Dugas M, Mergenthaler S, et al. Acute myeloid leukemias with reciprocal rearrangements can be distinguished by specific gene expression profiles. Proc Natl Acad Sci USA 2002;99:10008–13.
[18] Joyner DE, Bastar JD, Randall RL. Doxorubicin induces cell senescence preferentially over apoptosis in the FU-SY-1 synovial sarcoma cell line. J Orthop Res 2006;24:1163–9.
[19] Martinez N, Sanchez-Beato M, Carnero A, Moneo V, Tercero JC, Fernandez I, et al. Transcriptional signature of Ecteinascidin 743 (Yondelis, Trabectedin) in human sarcoma cells explanted from chemo-naive patients. Mol Cancer Ther 2005;4:814–23.
[20] Folmer F, Harrison WT, Tabudravu JN, Jaspars M, Aalbersberg W, Feussner K, et al. NF-kappaB-inhibiting naphthopyrones from the Fijian echinoderm Comanthus parvicirrus. J Nat Prod 2008;71:106–11.
[21] Kashman Y, Rudi A. The 13C-NMR spectrum and stereochemistry of heteronemin. Tetrahedron 1977;33:2997–8.
[22] Smyth GK. Linear models and empirical bayes methods for assessing differential expression in microarray experiments. Stat Appl Genet Mol Biol 2004;3. Article 3.
[23] Gentleman RC, Carey VJ, Bates DM, Bolstad B, Dettling M, Dudoit S, et al. Bioconductor: open software development for computational biology and bioinformatics. Genome Biol 2004;5:R80.
[24] Smyth G. Limma: linear models for microarray data. In: Gentleman R, Carey V, Dudoit S, Irizarry R, Huber W, editors. Bioinformatics and computational biology solutions using R and bioconductor. New York: Springer; 2005. p. 397–420.
[25] Smyth GK, Speed T. Normalization of cDNA microarray data. Methods 2003;31:265–73.
[26] Ritchie ME, Diyagama D, Neilson J, van Laar R, Dobrovic A, Holloway A, et al. Empirical array quality weights in the analysis of microarray data. BMC Bioinform 2006;7:261.

[27] Benjamini Y, Hochberg Y. Controlling the false discovery rate: a practical and powerful approach to multiple testing. JR Statist Soc B 1995;57:289–300.
[28] Kanehisa M, Goto S, Kawashima S, Okuno Y, Hattori M. The KEGG resource for deciphering the genome. Nucleic Acids Res 2004;32:D277–80.
[29] Draghici S, Khatri P, Tarca AL, Amin K, Done A, Voichita C, et al. A systems biology approach for pathway level analysis. Genome Res 2007;17:1537–45.
[30] Falcon S, Gentleman R. Using GOstats to test gene lists for GO term association. Bioinformatics 2007;23:257–8.
[31] Ashburner M, Ball CA, Blake JA, Botstein D, Butler H, Cherry JM, et al. Gene ontology: tool for the unification of biology. The Gene Ontology Consortium. Nat Genet 2000;25:25–9.
[32] Frith MC, Fu Y, Yu L, Chen JF, Hansen U, Weng Z. Detection of functional DNA motifs via statistical over-representation. Nucleic Acids Res 2004;32:1372–81.
[33] Wakaguri H, Yamashita R, Suzuki Y, Sugano S, Nakai K. DBTSS: database of transcription start sites, progress report 2008. Nucleic Acids Res 2008;36: D97–101.
[34] Suzuki Y, Yamashita R, Nakai K, Sugano S. DBTSS: DataBase of human transcriptional start sites and full-length cDNAs. Nucleic Acids Res 2002;30:328–31.
[35] Matys V, Kel-Margoulis OV, Fricke E, Liebich I, Land S, Barre-Dirrie A, et al. TRANSFAC and its module TRANSCompel: transcriptional gene regulation in eukaryotes. Nucleic Acids Res 2006;34:D108–10.
[36] Duvoix A, Delhalle S, Blasius R, Schnekenburger M, Morceau F, Fougere M, et al. Effect of chemopreventive agents on glutathione S-transferase P1-1 gene expression mechanisms via activating protein 1 and nuclear factor kappaB inhibition. Biochem Pharmacol 2004;68:1101–11.
[37] Cerella C, Scherer C, Cristofanon S, Henry E, Anwar A, Busch C, et al. Cell cycle arrest in early mitosis and induction of caspase-dependent apoptosis in U937 cells by diallyltetrasulfide (Al2S4). Apoptosis 2009;14:641–54.
[38] Folmer F, Blasius R, Morceau F, Tabudravu J, Dicato M, Jaspars M, et al. Inhibition of TNFalpha-induced activation of nuclear factor kappaB by kava (*Piper methysticum*) derivatives. Biochem Pharmacol 2006;71:1206–18.
[39] Hietakangas V, Poukkula M, Heiskanen KM, Karvinen JT, Sistonen L, Eriksson JE. Erythroid differentiation sensitizes K562 leukemia cells to TRAIL-induced apoptosis by downregulation of c-FLIP. Mol Cell Biol 2003;23:1278–91.
[40] D'Acquisto F, Lanzotti V, Carnuccio R. Cyclolinteinone, a sesterterpene from sponge Cacospongia linteiformis, prevents inducible nitric oxide synthase and inducible cyclo-oxygenase protein expression by blocking nuclear factor-kappaB activation in J774 macrophages. Biochem J 2000;346(Pt 3):793–8.
[41] Choi HJ, Choi YH, Yee SB, Im E, Jung JH, Kim ND. Ircinin-1 induces cell cycle arrest and apoptosis in SK-MEL-2 human melanoma cells. Mol Carcinog 2005;44:162–73.
[42] Jiang Y, Ahn EY, Ryu SH, Kim DK, Park JS, Kang SW, et al. Mechanism of cell cycle arrest by (8E,13Z,20Z)-strobilinin/(7E,13Z,20Z)-felixinin from a marine sponge *Psammocinia* sp.. Oncol Rep 2005;14:957–62.
[43] Rungeler P, Castro V, Mora G, Goren N, Vichnewski W, Pahl HL, et al. Inhibition of transcription factor NF-kappaB by sesquiterpene lactones: a proposed molecular mechanism of action. Bioorg Med Chem 1999;7:2343–52.
[44] Garcia-Pineres AJ, Lindenmeyer MT, Merfort I. Role of cysteine residues of p65/NF-kappaB on the inhibition by the sesquiterpene lactone parthenolide and N-ethyl maleimide, and on its transactivating potential. Life Sci 2004;75:841–56.
[45] Wonganuchitmeta SN, Yuenyongsawad S, Keawpradub N, Plubrukarn A. Antitubercular sesterterpenes from the Thai sponge *Brachiaster* sp.. J Nat Prod 2004;67:1767–70.
[46] Morotti A, Cilloni D, Pautasso M, Messa F, Arruga F, Defilippi I, et al. NF-kB inhibition as a strategy to enhance etoposide-induced apoptosis in K562 cell line. Am J Hematol 2006;81:938–45.
[47] Kefaloyianni E, Gaitanaki C, Beis I. ERK1/2 and p38-MAPK signalling pathways, through MSK1, are involved in NF-kappaB transactivation during oxidative stress in skeletal myoblasts. Cell Signal 2006;18:2238–51.
[48] Huang L, Chen CH. Proteasome regulators: activators and inhibitors. Curr Med Chem 2009;16:931–9.
[49] Richardson PG, Barlogie B, Berenson J, Singhal S, Jagannath S, Irwin D, et al. A phase 2 study of bortezomib in relapsed, refractory myeloma. N Engl J Med 2003;348:2609–17.
[50] Ruiz S, Krupnik Y, Keating M, Chandra J, Palladino M, McConkey D. The proteasome inhibitor NPI-0052 is a more effective inducer of apoptosis than bortezomib in lymphocytes from patients with chronic lymphocytic leukemia. Mol Cancer Ther 2006;5:1836–43.
[51] Schroder HC, Steffen R, Wenger R, Ugarkovic D, Muller WE. Age-dependent increase of DNA topoisomerase II activity in quail oviduct; modulation of the nuclear matrix-associated enzyme activity by protein phosphorylation and poly(ADP-ribosyl)ation. Mutat Res 1989;219:283–94.